

## Phase Diagram of Carbon Dioxide: Evidence for a New Associated Phase

Valentin Iota and Choong-Shik Yoo

*Lawrence Livermore National Laboratory, Livermore, California 94551*

(Received 18 January 2001)

The stability of CO<sub>2</sub> phases has been investigated up to 50 GPa and 750 K by *in situ* Raman spectroscopy and visual observations using externally heated diamond-anvil cells. A new phase (CO<sub>2</sub>-II) exists above 20 GPa and 500 K, which can be quenched to ambient temperature. The vibrational spectrum of this new CO<sub>2</sub> polymorph suggests the dimeric pairing of molecules. Based on the present *in situ* data and previous laser-heating results, we present new constraints for the phase diagram of carbon dioxide to 50 GPa and 2000 K. We find that carbon dioxide exhibits dramatic changes, both in the molecular configuration and in the nature of intermolecular interaction at high pressures and temperatures.

DOI: 10.1103/PhysRevLett.86.5922

PACS numbers: 64.70.Kb, 62.50.+p, 81.30.-t

The study of phase stabilities of molecular solids at high pressures and temperatures is important to understanding the nature of chemical bonding, intermolecular interactions, and collective behavior of molecules in condensed phases. Carbon dioxide (CO<sub>2</sub>) is a nearly chemically inert, simple linear molecule and is one of the important simple oxides in nature. Early high pressures studies established the existence of two molecular solid phases of CO<sub>2</sub>: a cubic (*Pa3*) phase I [1–3] and an orthorhombic (*Cmca*) phase III [4,5], both stabilized by quadrupolar interactions between the linear molecules [6]. In addition, two other polymorphs have been quenched from laser heated samples: a bent-molecular phase IV [7] between 10 and 30 GPa and a polymeric phase V [8] with a SiO<sub>2</sub>-tridymite-like structure (*P2<sub>1</sub>2<sub>1</sub>2<sub>1</sub>*) [9] above 40 GPa. In this study, we determine the stability of the CO<sub>2</sub> phases up to 50 GPa and 750 K, by using *in situ* Raman spectroscopy and visual observations in externally heated diamond-anvil cells. We report the discovery of a new phase, CO<sub>2</sub>-II [10], above 20 GPa and 500 K, whose vibrational spectrum indicates dimeric pairing of molecules.

The samples were loaded into a diamond-anvil cell by liquefying CO<sub>2</sub> (99.99% purity) at 233 K and 1 MPa in a high-pressure vessel. A resistive heater (Omega), capable of heating the sample to 750 K at pressures up to 50 GPa, was wrapped around the cell. The sample temperature was measured with a precision of ~1 K by using a calibrated thermocouple (*K*-type) in contact with the diamond anvils. A small amount of H<sub>2</sub>/Ar mixture (1% H<sub>2</sub>) was continuously flowed to avoid diamond oxidation above 600 K. A few micron-sized ruby (Al<sub>2</sub>O<sub>3</sub>:Cr<sup>3+</sup>) crystals were loaded in the cell, and the pressure was determined based on previously reported temperature-adjusted ruby luminescence [12]. Eleven heating experiments were performed by compressing the CO<sub>2</sub> samples to pressures up to 50 GPa, followed by heating to 750 K. Raman spectra were collected every 5 K, or even every 1–2 K near phase boundaries. Both the pressure and the temperature were monitored during heating. The pressure was found to decrease up to 20% during heating to the maximum tem-

perature of 750 K, presumably due to softening and/or relaxation of the diamond-anvil cell apparatus at high temperature.

The stability domains of CO<sub>2</sub> phases are summarized in Fig. 1. At ambient temperature, carbon dioxide crystallizes into an optically isotropic cubic (*Pa3*) phase I at 0.5 GPa [1–3]. CO<sub>2</sub>-I is a typical linear molecular solid with weak quadrupolar intermolecular interactions [6] and low (12 GPa) bulk modulus [9]. Above 12 GPa, it transforms to an orthorhombic (*Cmca*) phase III [4,5], which remains stable to 80 GPa [9]. The I → III transition is sluggish at ambient temperature; both phases coexist over an extended pressure range between 12 and 22 GPa [5]. In this study, we find that heating mixtures to 400 K eliminates all traces of the low-pressure phase I and thus fully stabilizes the high-pressure phase III. Above 400 K, the I → III transition occurs abruptly within 1–2 GPa without significant hysteresis. This result suggests that only CO<sub>2</sub>-III is stable above 12 GPa, without the presence of

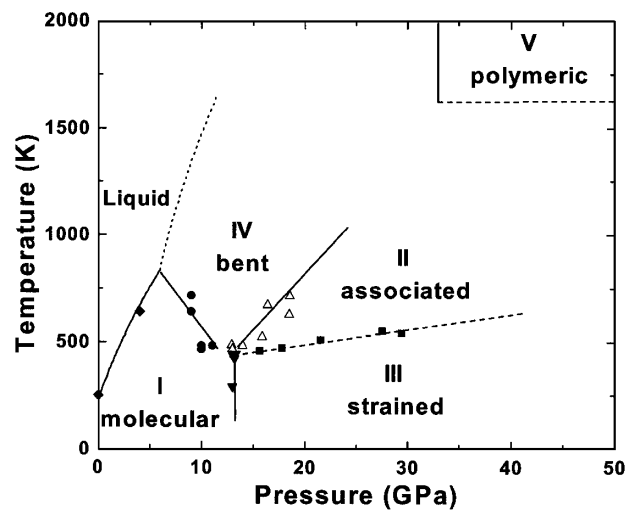


FIG. 1. The constraints for the phase diagram of CO<sub>2</sub>, based on the present *in situ* Raman measurements (data points) and on previous laser-heating experiments [7,8]. A new phase II is stabilized above 12 GPa and ~500 K.

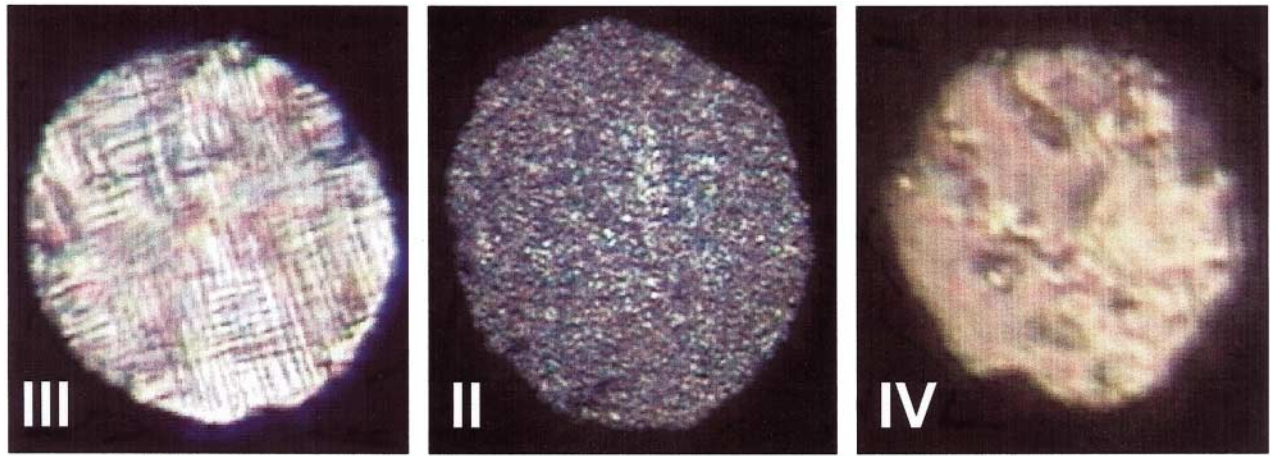


FIG. 2 (color). *In situ* microphotographs of three CO<sub>2</sub> phases: III at 450 K and 18.5 GPa, II at 610 K and 18 GPa, and IV at 720 K at 18.5 GPa. Orthorhombic CO<sub>2</sub>-III is optically anisotropic and shows a characteristic texture due to high lattice strain even at elevated temperatures. In contrast, the new CO<sub>2</sub>-II appears translucent and highly polycrystalline, and the bent-molecular phase IV is highly transparent and optically isotropic. The yellow tint of phase IV is due to thermal radiation at high temperature.

another “distorted cubic phase” previously proposed in this pressure range [13]. The extended metastability of cubic CO<sub>2</sub>-I to 22 GPa is likely due to its small energy difference from CO<sub>2</sub>-III in this pressure range [11]. The I → III phase transition also occurs without a discrete volume change in the specific volume [9].

CO<sub>2</sub>-III is not typical for a molecular solid, evident from its highly strained lattice (Fig. 2) with large pressure gradients (~100 GPa/mm at 30 GPa) and high bulk modulus of 80 GPa [9] (comparable to that of Si—87 GPa [14]). Above ~500 K at 19 GPa, it transforms to a new phase, CO<sub>2</sub>-II, as is apparent from distinct changes in both visual appearance (Fig. 2) and Raman spectrum (Fig. 3). The transition from CO<sub>2</sub>-III to II occurs sharply on heating (within 10 K) and is not reversible on lowering the temperature. As a result, CO<sub>2</sub>-II can be recovered at ambient temperature above 10 GPa.

Above 720 K at 19 GPa, CO<sub>2</sub>-II converts to the bent molecular CO<sub>2</sub>-IV (Figs. 2 and 3). CO<sub>2</sub>-IV has been discovered recently by laser heating CO<sub>2</sub>-III above 1000 K and 12 GPa [7], but the present study provides the first *in situ* evidence of its stability at high temperatures. The reverse transition (from IV to II) occurs rather slowly (minutes) and only in a narrow range of temperatures (~20 K) below the II ↔ IV transformation line. This explains why CO<sub>2</sub>-IV (instead of II) was quenched during the previous laser-heating experiments [7].

Previous studies show that the polymeric phase V is also quenchable at room temperature and is metastable over a wide range of pressures at 300 K [8]. As a result, above 12 GPa at room temperature, CO<sub>2</sub> can exist in any of four different phases (II, III, IV, and V) depending on the sample history. We emphasize that phases II, IV, and V are stable thermodynamically, since they always form at their stability conditions (shown in Fig. 1) regardless of the path followed. The same argument holds for CO<sub>2</sub>-I, as

the other four phases (II, III, IV, and V) revert to CO<sub>2</sub>-I below 8–10 GPa. In contrast, CO<sub>2</sub>-III appears only via the low-temperature compression of CO<sub>2</sub>-I, suggesting that CO<sub>2</sub>-III is likely a metastable phase. This implies that the

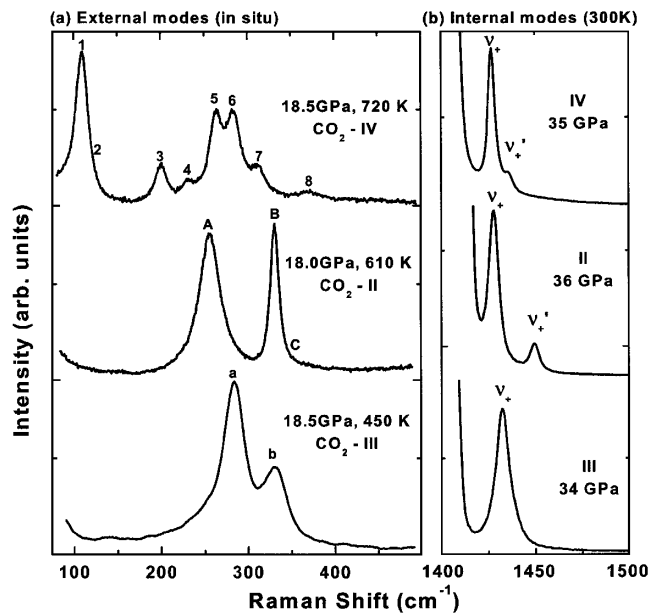


FIG. 3. Raman spectra of CO<sub>2</sub> phases II, III, and IV: (a) External modes, measured *in situ* at temperatures within their respective stability domains. The broad Raman bands of CO<sub>2</sub>-III suggest that the large lattice strain persists even at 450 K, consistent with its visual appearance in Fig. 2. The Raman spectrum of the new phase II is dominated by two strong and rather sharp bands, A and B, attributed to the characteristic vibrations of the (CO<sub>2</sub>)<sub>2</sub> pair. The spectrum of phase IV consists of eight distinct lattice modes suggesting a low symmetry structure (Ref. [7]). (b) Internal modes of phases III, II, and IV, measured from samples quenched at room temperature. The large splitting of the symmetric mode in CO<sub>2</sub>-II is viewed as evidence of pairing of the CO<sub>2</sub> molecules.

III  $\rightarrow$  II phase boundary may represent a kinetic barrier, rather than a thermodynamical phase boundary.

The phase diagram in Fig. 1 is extended to 50 GPa and 2000 K by adding the stability domain of phase V as determined by the previous laser-heating experiments [7,8]. The melting curve is based on the ambient melting point 190 K, the previous low-pressure melting data [15,16], and the present data at 640 K at 4 GPa. Note that four different phases (I, II, III, and IV) appear to be stable in the vicinity of the same pressure-temperature point ( $12 \pm 1$  GPa,  $480 \pm 5$  K). One way to reconcile this result with the Gibbs phase rule [17] would be to assume the existence of two distinct triple points separated by less than the present experimental precision (5 K and 1 GPa). However, a more likely explanation is that, as mentioned above, the III-II phase boundary represents a kinetic line of transition. This would extend the  $P$ - $T$  domain in which CO<sub>2</sub>-III can survive metastably to higher temperatures and contribute to the apparent singularity in the phase diagram.

Figure 3(b) compares the internal Raman modes of the three phases considered. In CO<sub>2</sub>-II, the internal  $\nu_+$  mode is split into two well-defined branches, whose separation rapidly increases with pressure (Fig. 4). At 40 GPa it exceeds  $25 \text{ cm}^{-1}$ , substantially larger than that expected for crystal field splitting (typically less than  $5 \text{ cm}^{-1}$  at 40 GPa

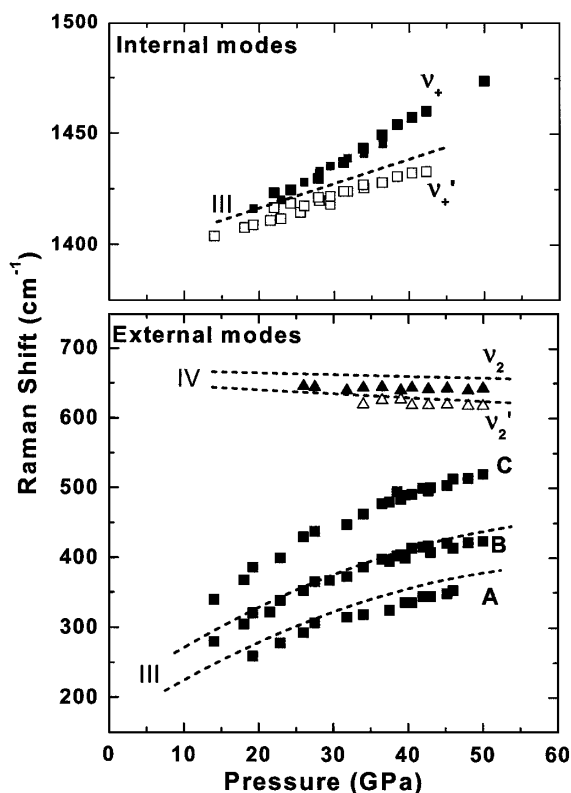


FIG. 4. Pressure shifts of the Raman modes of CO<sub>2</sub>-II at room temperature. The large split in the Fermi resonance band  $\nu_+$  is attributed to the dimeric pairing of CO<sub>2</sub> molecules in phase II. The dotted lines represent the corresponding Raman bands measured in CO<sub>2</sub>-IV presented for comparison.

as in the cases of CO<sub>2</sub>-III and IV, as shown in Fig. 2). The large  $\nu_+$  splitting in CO<sub>2</sub>-II is likely due to strong electrostatic dipole interactions, resulting from charge transfer between neighboring molecules. The energy separation between the lowest unoccupied molecular orbital ( $2\pi_u^*$ ) and the highest occupied molecular orbital ( $1\pi_g$ ) of CO<sub>2</sub> rapidly collapses with decreasing intermolecular distance and C-O-C angle [18]. Therefore, it is likely that the charge transfer occurs from nonbonding  $1\pi_g$  to antibonding  $2\pi_u^*$ , resulting in a partial destruction of  $\pi$  bonding and in a bent molecular configuration. The molecular bending of the O=C=O units in CO<sub>2</sub>-II is evident from the emergence of the  $\nu_2$  bending mode at  $650 \text{ cm}^{-1}$  (Fig. 4).

The pairwise association of CO<sub>2</sub> molecules splits all internal modes ( $\nu_s$ ,  $\nu_a$ , degenerated  $\nu_b$ ), and thereby its Fermi resonance  $\nu_+$  mode, into two modes (*in-phase* and *out-of-phase*):  $3A_g + 3B_u + 1A_u + 1B_g$ . In addition, it generates four new additional modes associated with CO<sub>2</sub>  $\cdots$  CO<sub>2</sub> dimeric vibrations:  $\nu_s(A_g)$ ,  $\nu_a(B_u)$ ,  $\nu_b(A_g)$ , and  $\nu_b(A_u)$ .

The layered crystal structure of CO<sub>2</sub>-III ( $Cmca$ ) offers a nearly perfect arrangement for electron charge transfer from intramolecular to intermolecular bonds and thereby for dimeric association of molecules. At relatively low pressures, carbon dioxide is highly compressible (35% volume compression at 20 GPa) [9]. As a result, the nearest interatomic carbon-oxygen distance of CO<sub>2</sub>-III collapses to  $2.582 \text{ \AA}$  in a “T-shape” ( $C_{2v}$ ) configuration within the basal  $c$  plane or to  $2.610 \text{ \AA}$  in a side-by-side “staggered” ( $C_{2h}$ ) configuration along the  $c$  axis. Both of these distances are only slightly greater than twice the C=O bond distance of  $1.114 \text{ \AA}$  [9]. In CO<sub>2</sub>-I, where the intermolecular interaction is strictly quadrupolar, the nearest C  $\cdots$  O ( $3.144 \text{ \AA}$ ) and O  $\cdots$  O ( $3.211 \text{ \AA}$ ) interatomic distances are significantly larger. The vibrational frequencies of CO<sub>2</sub> dimer have been calculated in a staggered configuration with the interatomic C  $\cdots$  O distance of  $2.900 \text{ \AA}$ , resulting in the symmetric deformation and breathing modes at  $75$  and  $179 \text{ cm}^{-1}$ , respectively [19]. These calculated frequencies are in good agreement with those of the measured peaks (A and B) extrapolated to ambient pressure ( $110$  and  $180 \text{ cm}^{-1}$ ) in Fig. 4. Recent calculations of the valence charge distribution in the  $C_{2h}$  dimer of CO<sub>2</sub> also predict an increased electron density in the region between the molecules [20]. Importantly, similar charge transfer dimers have also been observed in CS<sub>2</sub> [21], H<sub>2</sub>-III [22], O<sub>2</sub> [23], Li<sub>2</sub> [24], and halides [25] at high pressures. It is also remarkable to note that those transitions occur also from a  $Cmca$  or analogous crystal structure [21–26].

In conclusion, we have presented new constraints for the phase diagram of carbon dioxide and evidence for a new dimeric polymorph CO<sub>2</sub>-II. Carbon dioxide exhibits a rich polymorphism at high pressures and temperatures with phases differing greatly in molecular configuration, intermolecular interaction, and chemical bonding. The stability

of the phases can be understood systematically in terms of pressure-induced electron delocalization, resulting from a stronger density dependence of the repulsive electron kinetic energy ( $\rho^{-2/3}$ ) than of the electrostatic potential energy ( $-\rho^{-1/3}$ ). Such increased electron delocalization leads to a gradual convergence of the strengths of *intra-molecular* and *intermolecular* interactions and to transformations of the molecular-solid phase I to more electron delocalized structures such as strained-III, dimeric-II, bent-IV, and eventually extended-V. In turn, the occurrence of these new phases with partially delocalized electrons softens the repulsive potentials and retards the insulator-metal transition in carbon dioxide.

We thank H. Cynn and K. Visbeck for help with the experiments. This work has been supported by the LDRD and PDRP programs at the Lawrence Livermore National Laboratory, University of California, under the auspices of the U.S. Department of Energy under Contract No. W-7405-ENG-48.

- 
- [1] P.W. Bridgeman, Proc. Am. Acad. Arts Sci. **72**, 207 (1938).
- [2] R.C. Hanson and L.H. Jones, J. Chem. Phys. **75**, 1102 (1981).
- [3] B. Olinger, J. Chem. Phys. **77**, 6255 (1982).
- [4] R.C. Hanson, J. Phys. Chem. **89**, 4499 (1985).
- [5] K. Aoki *et al.*, Science **263**, 356 (1994).
- [6] B. Kuchta and R. Eters, Phys. Rev. B **47**, 14 691 (1993).
- [7] C.-S. Yoo, V. Iota, and H. Cynn, Phys. Rev. Lett. **86**, 444 (2001).
- [8] V. Iota, C.-S. Yoo, and H. Cynn, Science **383**, 1510 (1998).
- [9] C.-S. Yoo, H. Cynn, F. Gygi, G. Galli, V. Iota, M. Nicol, S. Carlson, D. Hausermann, and C. Mailhot, Phys. Rev. Lett. **83**, 5527 (1999).
- [10] This phase is different from the CO<sub>2</sub>-II proposed by Liu to exist between 0.5–2.3 GPa [L. Liu, Nature (London) **303**, 508 (1983)]. That assignment has been disputed by a number of recent reports [2,5–7,11] that find no evidence of a phase transition in that pressure range.
- [11] F. Gygi, Comput. Mater. Sci. **10**, 822 (1998).
- [12] J. Yen and M. Nicol, J. Appl. Phys. **72**, 5535 (1992).
- [13] H. Olijnyk and A. P. Jephcoat, Phys. Rev. B **57**, 879 (1998).
- [14] E. Knittle, *Handbook of Physical Constants*, edited by T. Ahrens (American Geophysical Union, Washington, DC, 1995), pp. 98–142.
- [15] H. Shimizu, K. Kitagawa, and S. Sasaki, Phys. Rev. B **47**, 11 567 (1993).
- [16] R. Span and W. Wagner, J. Phys. Chem. Ref. Data **25**, 1509 (1996).
- [17] The Gibbs phase rule limits the number of *thermodynamically stable* phases that can coexist at a point in the *P-T* space. See G.W. Castellan, in *Physical Chemistry—Second Edition* (Addison-Wesley, Reading, MA, 1971), pp. 277–281.
- [18] A. D. Walsh, J. Chem. Soc. (London) **III**, 2260 (1953); **III**, 2266 (1953); also see G. Herzberg, *Molecular Spectra and Molecular Structure* (Van Nostrand Reinhold, New York, 1966), Vol. III, p. 312.
- [19] A. J. Illies, M. L. McKee, and H. B. Schlegel, J. Phys. Chem. **91**, 3489 (1987).
- [20] B. Holm, R. Ahuja, A. Belonoshko, and B. Johansson, Phys. Rev. Lett. **85**, 1258 (2000).
- [21] S. F. Agnew, R. E. Mischke, and B. I. Swanson, J. Phys. Chem. **92**, 4201 (1988).
- [22] R. J. Hemley, Z. G. Soos, M. Hanfland, and H. K. Mao, Nature (London) **369**, 384 (1994).
- [23] F. A. Gorelli, L. Ulivi, M. Santoro, and R. Bini, Phys. Rev. Lett. **83**, 4093 (1999).
- [24] J. B. Neaton and N. W. Ashcroft, Nature (London) **400**, 141 (1999).
- [25] Y. Fujii, K. Hase, Y. Ohishi, H. Fujihisa, N. Hamaya, K. Takemura, O. Shimomura, T. Kikegawa, Y. Amemiya, and Y. Matsushita, Phys. Rev. Lett. **63**, 536 (1989).
- [26] B. Edwards, N. W. Ashcroft, and T. Lenosky, Europhys. Lett. **34**, 519 (1996); H. Kitamura, S. Tsuneyuki, T. Ogitsu, and T. Miyaki, Nature (London) **404**, 259 (2000); A. K. McMahan and M. Ross, Phys. Rev. B **15**, 718 (1977).